Superconducting Hybrid Fault Current Limiter: Manufacturing, Modelling and Simulations

E. OYARBIDE USABIAGA
MONDRAGON UNIBERTSITATEA
Loramendi 4, Apdo. 23
20500 Mondragón
SPAIN
eoyarbide@eps.muni.es

F. GIL GARCIA
SCHNEIDER ELECTRIC
4, rue Volta
F-38050 Grenoble cedex 9
FRANCE
francisco_gil-garcia@mail.schneider.fr

L. GARCÍA-TABARÉS
CIEMAT
Avda Complutense, 22
E 28040 Madrid
SPAIN
LuisGT@ciemat.es

J.L. PERAL
R. ITURBE
ANTEC
Ramon y Cajal, 74
E 48920 Portugalete ,
SPAIN

J.M. RODRÍGUEZ
E. URRETAVIZCAYA
RED ELECTRICA DE ESPAÑA
Pº del Conde de los Gaitanes 177
28109 La Moraleja,.Alcobendas,
SPAIN, rodgarju@ree.es,

P. MARTINEZ CID
IBERDROLA
Gardoqui 8
48008 Bilbao
SPAIN
pedro.mcid@iberdrola.es

X. GRANADOS
ICMAB, Universidad
Autónoma de Barcelona
E08193 Barcelona
SPAIN
Granados@icmab.es

Abstract - **This paper presents the work that is being done as a part of the ByFault project (Brite/Euram projet finaced by the European Community): manufacturing, modelling and simulation of a Superconducting Hybrid Fault Current Limiter (SHFCL). The SHFCL is based on a variable impedance transformer: primary winding is in series with the protected line and several secondaries are short-circuited by superconducting elements. This topology has been modelled using 2D and 3D finite elements, and some useful formulation to simulate the behaviour of the SHFCL has been obtained. The SHFCL's integration with the electrical network has been simulated using several tools (ATP-EMTP, PSS/E and Power System Blockset of Matlab), depending on the application and the desired location voltage.**

Keywords: Superconducting fault current limiter, manufacturing, modelling, bus-bar connection

I. INTRODUCTION

The main idea behind a High Voltage Superconducting Fault Current Limiter (HVSFCL) is that in normal state (superconducting state) the HVSFCL has an almost negligible impedance while during the fault, the existence of high currents induces the lost of the superconducting state and the HVSFCL's impedance increases abruptly. The advantage of this kind of device face to the classical current limiter resides in its very fast operation capability with a real current peak limitation.

One of the planned HVSFCL will be resistive [1]. A superconducting element is placed in series with the network, showing a zero-impedance behaviour during normal state and a current limiting resistance during the fault. The second planned HVSFCL will be hybrid [2]. The SHFCL is based on a variable impedance transformer: primary winding is in series with the protected line and several secondaries are short-circuited by superconducting elements. As the flux is constrained to zero in normal state the impedance of the primary is composed only by leakage inductance. In a fault occurrence case the resistance of all the secondaries increase and a current limiting inductive behaviour (due to the magnetising inductance) is observed from the primary.

Both HVSFCL have been successfully tested in a laboratory environment. In order to insert the device in a MV network previous theoretical study and simulations are needed. This paper describes some of this previous work related to the hybrid HVSFCL, including manufacturing, modelling, simulations and location choice.

II. SHFCL DESCRIPTION

The practical configuration of the One-Phase Hybrid Limiter is in the form of a toroidal transformer (Fig. 1), with the superconducting bars short-circuiting its N secondaries, and the primary connected in series to the network to be protected. Each secondary is a short-circuited ring formed by the series interconnection of a superconducting bar and a copper ring.

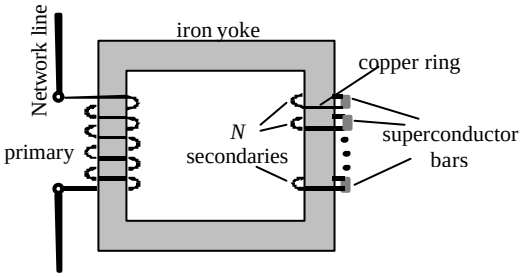

Fig. 1. General Scheme of the SHFCL.

The superconductor is melt textured YBCO 123 [2] in the shape of small rods which are cut to match the required dimensions. As the superconductor is working at 77K, all the secondary must be placed inside a cryostat. The fact that the copper of this winding is working at cold reduces considerably its electrical resistance and helps to achieve a lower impedance of the limiter at no-fault condition.

The device is placed in series with the network: in the event of a fault, when the primary current exceeds a certain value, the current through each bar will grow beyond the so called critical current and the superconductor will start

to transit to the resistive state. Triggering current of the limiter is defined by the transforming ratio of the limiter and the critical current of the bars.

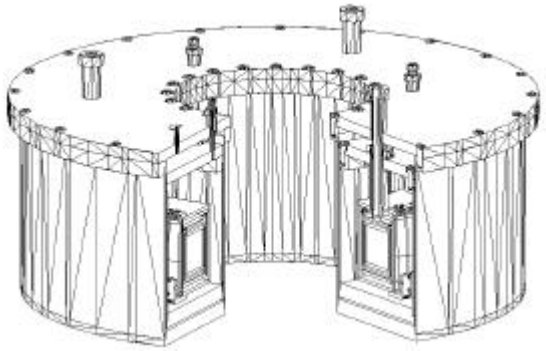

Fig. 2.a. General view of one-phase HVSFCL prototype.

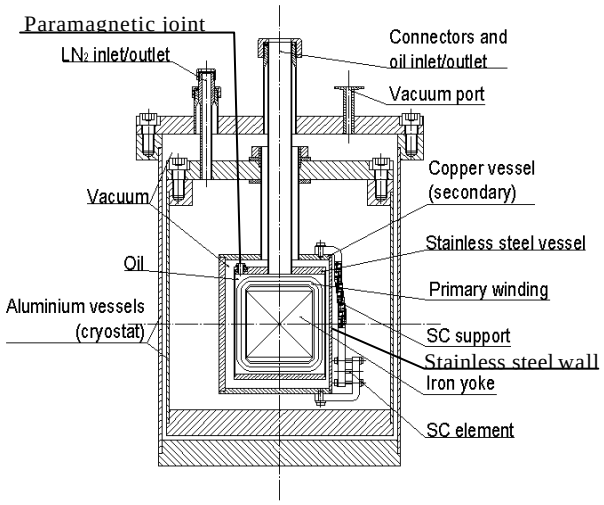

Fig. 2.b. Section of the HVSFCL.

The yoke is composed of 0.23mm thick laminated iron insulated by fiber glass and the primary winding is made of conventional copper. This winding is separated in three independent sections, so it is possible to test different voltage and limiting current configurations in the same prototype.

The primary winding is enclosed in an oil cooled vessel (Fig. 2). To get a high thermal insulation between primary (room temperature) and secondary (cryogenic temperature) circuits, a vacuum chamber insulation schema is proposed. In order to minimise prototype costs this vacuum chamber is composed by an internal stainless steel toroid and an external secondary toroid. As the internal metallic structure can confinate all the magnetic flux a paramagnetic joint has to be inserted in order to break the magnetic circuit.

The secondary toroid has a rectangular-shape section composed of three copper walls and one stainless steel high resistive wall. This stainless steel wall is short circuited by the superconducting elements. This elaborate structure achieves three goals: vacuum insulation, electrical secondary easy disposition and a shunt protecting resistance addition. A fiber glass wall has been used to reinforce the weak thick stainless steel wall. All the secondary is in a LN_2 bath, so at 77ºK.

Finally, another vacuum chamber isolates the secondary vessel from the outside.

III. SHFCL MODELLING

Under the previous considerations, the problem of analysing the behaviour of the limiter can be solved by means of an equivalent circuit, formally identical to that of the conventional transformer, with the only difference being the variable resistance of the secondary.

Basically there are two aspects to model; the magnetic and the thermoelectric one, which are finally coupled to provide the complete behaviour of the limiter under a fault.

Both models can be defined in terms of the equivalent circuit. The magnetic model should provide the values of the different inductances, while the thermoelectric model defines the variable resistance corresponding to the secondary winding. Fig. 3 shows the equivalent circuit of the SHFCL

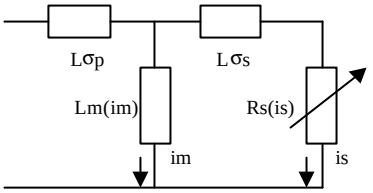

Fig. 3. Equivalent Circuit of the SHFCL.

A. Magnetic modelling

For a first estimate, simple analytical computations can be considered to evaluate leakage fluxes as well as the main flux, especially if saturation is neglected.

There are two leakage inductances corresponding to the primary and secondary magnetic circuits. As all the flux arising from the primary is embraced by the secondary, the primary leakage inductance can be neglected. The secondary leakage inductance takes into account the fraction of flux created by the secondary that does not reach the primary. For an ideal toroid, this flux can be calculated using the Ampere´s law, which provides the following value for the leakage inductance referred to the primary side:

$$L^{*}_{\sigma s} = \frac{\mu_0 \cdot S_{\sigma s} \cdot N_p^{\,2}}{l_h} \qquad (1)$$

where $S_{\sigma s}$ is the leakage area, l_h the iron length and N_p the number of primary turns.

Calculation of the magnetising inductance (corresponding to the mutual flux between both windings) is also very easy to compute when saturation is not taken into account and an ideal geometry is considered. Again application of Ampere´s law provides the following equation:

$$L_m = \frac{\mu_r \cdot \mu_0 \cdot S_h \cdot N_p^{\,2}}{l_h} \qquad (2)$$

where S_h is the iron cross section and μ_r its magnetic permeability. These analytical modelling results have been widely validated by 2D and 3D finite elements method.

While the assumption of no iron saturation is completely valid for the no-fault condition, as the secondary side is short-circuited, it can be absolutely unrealistic for the fault condition, when the secondary impedance is high and the full voltage is applied to the limiter. For a more accurate simulation, saturation must be considered, leading to a non-linear problem where the value of L_m depends on the magnetising current i_m. A certain simplification can be achieved if the primary resistance is neglected. As no primary leakage inductance is considered, all the supply voltage is applied to L_m so that the current trough this impedance can be easily found from the B-H iron curve.

B. Thermoelectric transition modelling

The state of the superconducting bars is represented by the parameter R_s of the electrical equivalent circuit.

Due to material's non-homogeneous nature, when the current in the superconductor bar crosses a certain value, only a limited number of points inside the bar (N_q) loss their superconducting state. The heat generated at these points propagates to the rest of the material and makes it transit to the normal state. It is a diffusion process governed by a differential equation and after some simplifications, a characteristic parameter of the problem can be found, the so called quench propagation velocity. Derivation of this parameter is out of the scope of this paper but this speed can be found using the equivalent electrical analogies of the process. Its expressions is given as:

$$v_q = \frac{J}{C_v}\sqrt{\frac{2K\tilde{n}}{\ddot{A}T_c}} \qquad (3)$$

where, K is the thermal conductivity, ρ the electrical resistivity, C_v the specific heat, J the current density flowing through it and ΔT_c the difference between critical temperature and bath temperature.

The resistance development is governed by the following set of equations

$$x(t) = N_q\int v_q dt = \frac{N_q}{S_b C_v}\sqrt{\frac{2K\tilde{n}}{\ddot{A}T_c}}\int I(t)dt \qquad (4.a)$$

$$R(t) = \rho(t)\cdot\frac{x(t)}{S_b} \qquad (4.b)$$

while the current evolution, I(t), will be computed from the equivalent circuit shown in Fig. 3 and the corresponding external conditions. S_b is the bar cross section.

The values for the physical constants of the superconducting material should be taken at critical temperature. Finally, the temperature at the "hot spot", ΔT, can be found from the following equation:

$$\int_0^{tf} I^2(t)dt = \int_{Ti}^{Tf}\frac{S^2_b\cdot C_v(T)}{\rho(T)}dT = S^2_b\cdot\delta\cdot\Delta T \qquad (5)$$

where δ is the $C_v/\rho(T)$ ratio. Equation (5) is important to know the temperature evolution, which provides the value of the resistivity to be used in (4.a).

From (4.b) it can be noticed that the higher the number of initial normal points, the higher the propagation speed and thus the lower the final temperature. So, to avoid superconductor bar destruction by overheating problems a high number of initial normal points will be desirable.

IV LOCATION IN THE NETWORK

The three-phase FCL will be first built and tested for medium voltage operation so this section will be focused in the device's location and its nominal values choice criteria.

A. Location in the network

A SFCL has two main properties: current limitation capability and ultra high-speed operation. The first capability is interesting if any network or element can not be well protected by traditional devices or if this protection is more expensive than a SFCL solution. By now, it is almost always possible to protect any power element with a suitable electromechanical device, and the SFCL price seems to be several times higher than classical solutions. What is more, with this series "over-protection" scheme the power quality received by the customer is not improved.

But in the other hand, ultra high-speed operation property seems to have a quite interesting application: parallel interconnection of existing isolated networks. Bus-bar connection (Fig. 4) is a good example of this.

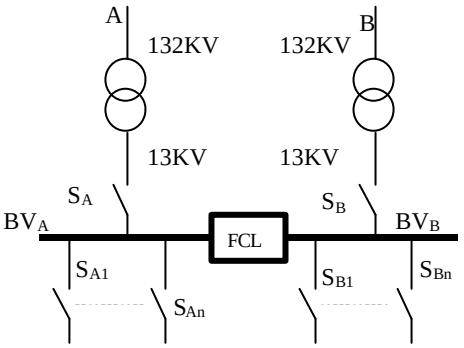

Fig. 4. FCL location

This interconnection improves overall reliability and voltage quality: non desired supply variations (i.e. harmonics) are damped, better energy distribution is achieved and in case of a short time supply fault in any of the two feeders the other one will feed all MV lines. The advantage of the SHFCL is the capability to do so without MV line fault propagation. Another benefit is that a new bus bar connection can be achieved with few protection rating changes. All this means that SFCL is not used for

"protection" tasks but for power quality improvement via a "Fault Rejecting Link".

B. Device's characteristic values: nominal current (I_n), quench current (I_q) and limited current (I_l).

The proposed bus-bar connection is located in Iberdrola's distribution network (Spain). After a 132KV/13.2KV transformer conversion a 13KV link is proposed. All the MV network and HV equivalents have been modelled in the MATLAB-Simulink environment (more than 150 nodes). In order to get the characteristic values several scenarios have been studied:

1) Normal operation: both bars are well fed and a small current passes across the device ($5A_{RMS}$).

2) HV source failure: any of the two HV lines or transformers is temporally disconnected and one feeder supplies both bus-bars via the SFCL. An important current passes across the device ($527A_{RMS}$). The nominal current must be over this current, so we can set $I_n = 700A_{RMS}$.

3) MV fault: a fault occurs in any of the lines of any of the two bus-bars. A fault current will began to pass across the SFCL. Depending of the fault location (in the beginning, midway or end of a line) the fault current will be different. In our simulations we have measured a $6500A_{RMS}$ fault for the lowest case (end of the line). The quench current must be under this fault current value, so the device will change of state and current limitation will be achieved. This way, we choose $I_q = 1500\sqrt{2}\,A$. As the fault must be "transparent" for the good-side protection system, the limited current must be below or equal to the nominal current, so $I_l = 700A_{RMS}$.

4) HV nearby fault: a HV fault occurs near the chosen location. A high fault current began to cross the FCL from the good source to the damaged one. This HV fault current should be much higher than MV one, so I_q is reached and the FCL quenches.

C. Fault occurrence simulation.

Fig. 5. shows a simulation with the related different states of the device: (I) normal state, without harmonics, the SFCL current is quasi-null; (II) HV occurrence, disconnection of HV source **A**, its bus-bar is fed by 2nd transformer, and so on, a $530A_{RMS}$ current crosses the SFCL; (III) HV occurrence is cleared and normal state is reached; (IV) MV fault, a fault occurs in the end of a line in the bus-bar **A**, The SFCL quenches and current is limited to $700A_{RMS}$.

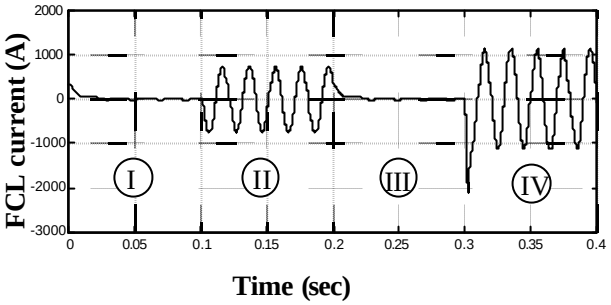

Fig. 5. SFCL current.

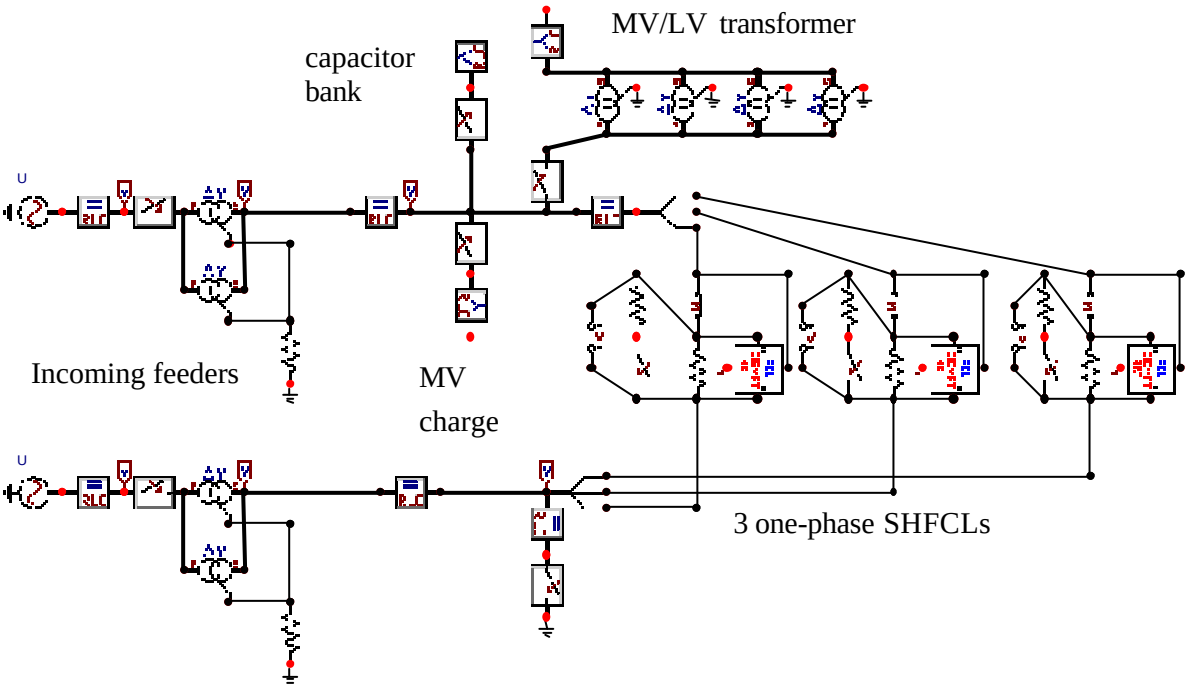

Fig. 6. Equivalent ATP-Draw circuit.

D. Non-desired quench.

FCL link behaves as a short circuit for any slight voltage gap between the two sources, making current to increase and FCL to quench unnecessarily. This way, voltage harmonics could be a non-desired quench origin, but simulations have shown that the harmonic power has to reach the 75% of nominal power to quench, something really impossible. In the other hand, transformer tap control could be a problem, as FCL ultra high operation capability makes classical synchronisation devices inoperable. To avoid this problem a switch is proposed in parallel with the FCL. It will be closed for tap change operation and opened for normal operation.

V. SWITCHING SIMULATIONS

The SHFCL numerical model described in chapter III has been introduced into numerical power grid models using simulation language MODELS [3] for EMTP-ATP [4] (Electromagnetic Transients Program – Alternating Transients Program).

The goal is to study the switching transient behaviour of the SHFCL in the power network. In this way, it will be possible to validate the SHFCL location in the network. Fig. 6 depicts the equivalent ATP-Draw [5] circuit of the main network studied. Joined to the bus bar we can find an overhead line, a MV charge, a capacitor bank and a low voltage charge through a MV/LV transformer.

Fig. 7 shows the short circuit current (in per unit value) with and without the contribution of a SHFCL.

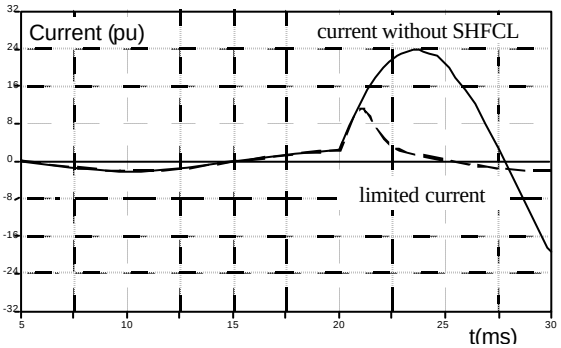

Fig. 7. Current limitation of a SHFCL.

When limiting in short circuit conditions, the transient overvoltage through the SHFCL can be higher than the phase to ground voltage. In order to reduce the transient voltage an impedance shunt can be added (Fig. 8).

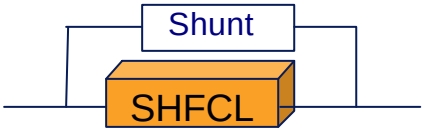

Fig. 8. Shunt impedance in a SHFCL.

Fig. 9 compares SHFCL's voltage level in three different scenarios: a) without shunt (solid) b) with an inductive shunt (dashed) c) with a resistive shunt (dotted).

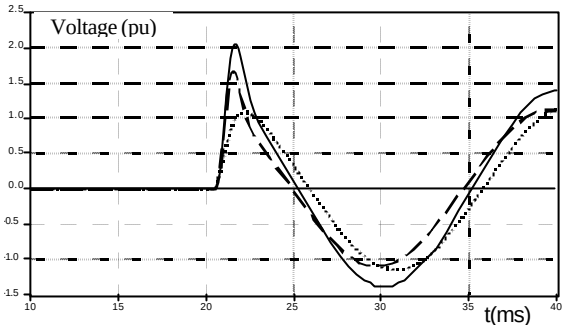

Fig. 9: Voltage in the SHFCL: a) without shunt (solid) b) with an inductive shunt (dashed) c) with a resistive shunt (dotted).

As expected, the best case is the resistive shunt one. Moreover, in this case the current zero-crossing point is delayed (Fig. 10).

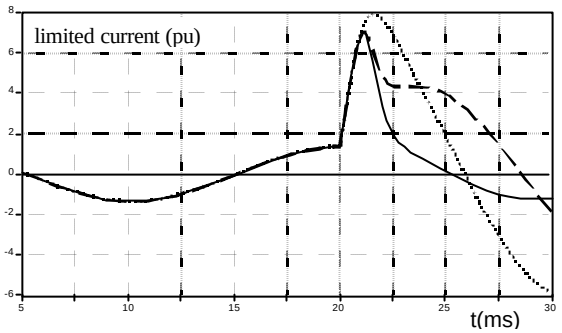

Fig. 10. Current through the SHFCL. a) without shunt (solid) b) with an inductive shunt (dashed) c) with a resistive shunt (dotted).

The chosen location does not show any damaging resonance value so a real test will be suitable. As the limited current is low enough, a cheap breaker will be able to cut the remaining current, and thanks to this short working period the resistive shunt cost will be low enough.

VI. HIGH VOLTAGE SIMULATIONS

The Byfault project perspectives does not include any HV implantation in next 2 years (remaining of the project). Nevertheless, we have considered interesting to get some results in SHFCL behaviour in HV scenario. This way an important work concerning the model “scaling rules” has been done. This work goes out of the scope of this paper so we will only show some simulations results.

For HV simulations an user defined PSS/E model has been developed in FLECS. A three-phase short circuit that lasts 100 milliseconds is considered. The short circuit is cleared correctly with a successful reclosing. In the first case, the SHFCL was placed in a 400 kV line. The goal was to decrease abruptly the short circuit current to allow old cutting devices (and/or bad dimensioning ones) to cut the lowered short circuit current.

Fig. 11 shows the current (I) through the line, without (dotted line) and with SHFCL (dashed line). The short circuit current is decreased few milliseconds after its presence and it is kept at a very low value until the fault is

cleared by the protection system. Another additional benefit is the diminution of the voltage sag produced by the fault (Fig. 12).

The second scenario is a HV bus-bar connection. Fig. 13 shows the current (I) through the line, without (dotted line) and with SHFCL (dashed line). The current through the SHFCL is very similar to the previous example: the short circuit current decreases drastically very quickly after the presence of the short circuit and it is kept at a very low value until the default is cleared by the protection system.

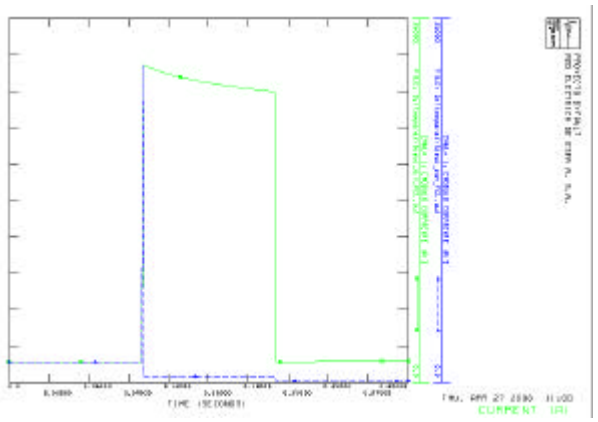

Fig. 11. Current (I) through the line

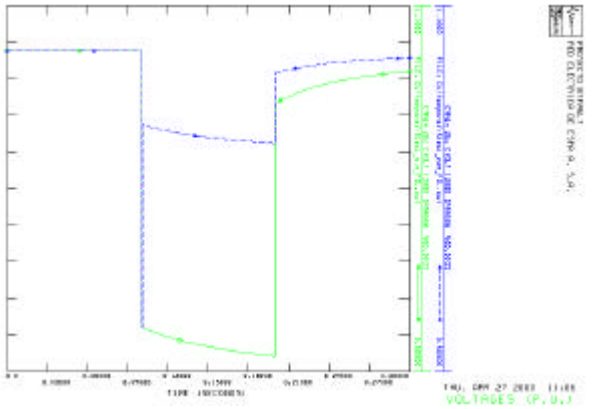

Fig. 12. Voltage (p.u.) at the connection point.

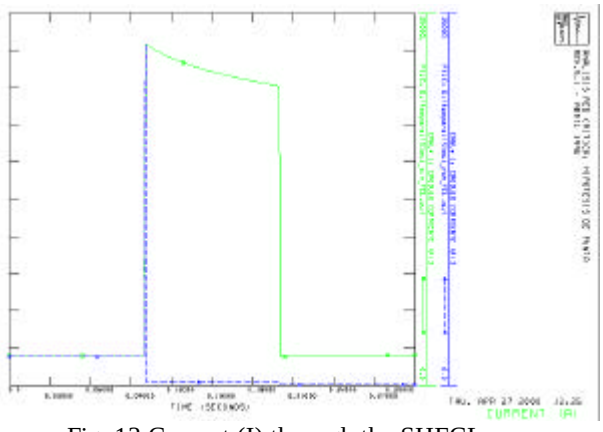

Fig. 13 Current (I) through the SHFCL

Fig. 14 depicts the "good bar" voltage. The sag is diminished thanks to the high-speed SHFCL operation. This way the very sensitive users are not affected.

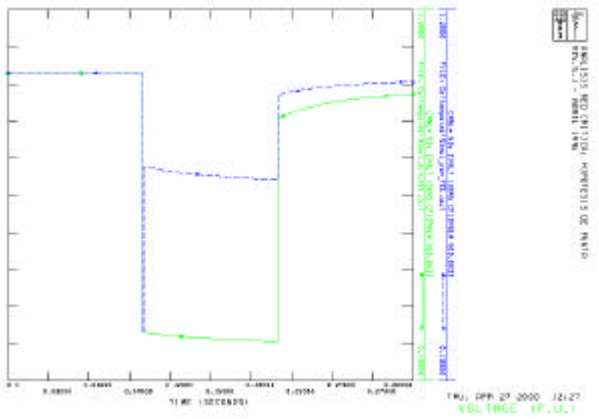

Fig, 14. Voltage (p.u.) at the "normal" substation side.

VI. CONCLUSIONS

A knowledge-based SHFCL state-space model has been developed and inserted in three different simulation tools. This state-space model takes into account hot spots generation and propagation. This way, device's actual behaviour could be accurately predicted.

Device's nominal values have been fixed, and some realistic simulations showing a non-destructive behaviour of the superconductor material have been carried out.

Bus-bar connection seems to be the best location, as there is no classical device's replacing needs, the SHFCL poor reclosing time is not a problem and only few protection rating changes have to be done. This way, an economic-optimal is achieved.

Further work will be focused in both economical and technological aspects; we have to know if this economically-optimal value is cheap enough and in the other hand, it is desirable to find the simplest "model scaling-rules"

VI. REFERENCES

[1] J. Noudem, J.M. Barbut, O. Belmont, J. Sanchez, P. Tixador, R. Tournier, "Current limitation at 1080 A under 1100 V with bulk Bi-2223", *IEEE Transactions on Applied Superconductivity*, Vol. 9, Nº2, pp. 664-667, June 1999

[2] X. Granados, X. Obradors, T. Puig, E. Mendoza, V. Gomis, S. Piñol, L. García Tabarés and J. Calero, "Hybrid superconducting fault current limiter based on bulk melt textured $Yba_2Cu_3O_7$ ceramic composites", *IEEE Transactions of Applied Superconductivity*, 9 (2), 1999, pp. 1308-1311

[3] L. Dubé, "Using the simulation language MODELS with EMTP", *Proc. 11th Power Systems Computation Conference, pp. 1063-1069 Avignon, 1993*

[4] Canadian-American EMTP Users Group, *Alternative Transients Program Rule Book*, 1998.

[5] L. Prikler, H. K. Hoidalen, *ATPDraw for Windows 3.1x/95/NT version 1, User's Manual*, SefAS TR A4790 Norway, ISBN 82-594-1358-2, Oct. 1998